World Academy of Science, Engineering and Technology
International Journal of Environmental and Ecological Engineering
Vol:9, No:7, 2015

CFD Simulations to Study the Cooling Effects of Different Greening Modifications

An-Shik Yang, Chih-Yung Wen, Chiang-Ho Cheng, Yu-Hsuan Juan

***Abstract*—**The objective of this study is to conduct computational fluid dynamic (CFD) simulations for evaluating the cooling efficacy from vegetation implanted in a public park in the Taipei, Taiwan. To probe the impacts of park renewal by means of adding three pavilions and supplementary green areas on urban microclimates, the simulated results have revealed that the park having a higher percentage of green coverage ratio (GCR) tended to experience a better cooling effect. These findings can be used to explore the effects of different greening modifications on urban environments for achieving an effective thermal comfort in urban public spaces.

***Keywords*—**CFD simulations, green coverage ratio, urban heat island, urban public park.

I. Introduction

AS urban development continues to increase, natural vegetation cover is being replaced with the constructed buildings and the infrastructure, forming a well-known heat island effect which can noticeably raise temperatures in densely built-up urban areas during the summer months. Urban parks are known to be useful for providing cool microclimates and mitigate the urban heat island (UHI) outcome attributable to the presence of vegetation cover. Various studies have been extensively conducted to utilize green space in moderating urban climates [1]. Researchers consistently suggested an effective way to alleviate the UHI effects via increasing tree cover area and density [2]. In recent times, the computational fluid dynamics (CFD) tool has become increasingly important to perform pre-evaluation and design simulations of quantitatively analyzing the cooling effect of green spaces in the development of urban planning. Several vegetation models were proposed and assessed in literature for reproducing the aerodynamic effect of trees on the airflow. In addition, to ease the urban heat island effect, Taha developed a vegetation model mainly classified as trees, green roofs and surfaces [3]. Bruse and Fleer utilized the microclimate CFD model, ENVI-met, to study the impact of ground coverage on thermal stress over a small park [4]. Dimoudi and Nikolopoulou employed CFD to address the cooling effect of different vegetation arrangements in a generic building setup [5]. Alexandri and Jones conducted the CFD studies to describe the thermal influences of green walls and green roofs on the microclimate for nine different climates and urban canyon geometries [6]. Fröhlich and Matzarakis used the ENVI-met software to analyze the impacts of urban street design and surface material on the human thermal comfort [7]. Besides, Vidrih and Medved validated a three-dimensional CFD model by comparing the measured results with the predicted air temperatures in tree crowns, demonstrating the sufficiency of proposed CFD procedure to correctly simulate the thermo-flow processes in the city park environment [8]. Srivanit and Hokao focused on the strategies of greening modification through adding more greening area, including an on-site measurement and a numerical simulation model that uses ENVI-met [9].

The goal of this research is to perform CFD simulations for assessing the vegetation efficiency of a public park (with different greening types, e.g. trees and plants, green roofs, vertical green walls and grass lawns) and its influence on the atmosphere of bordering locality in a densely urbanized area in Taipei, Taiwan, which has a hot and humid climate. Numerical simulations were extended to investigate the influences of adding three pavilions and supplementary green areas on urban microclimates during the park renewal. The findings of this research will support better prediction of the influences of park renewal and spatial arrangements of different greening modifications, helping urban planners and managers mitigate increasing temperatures associated with climate change as well as to achieve an effective thermal adaptation of urban public spaces.

II. Description of Building Model

Xinsheng Park in this research was part of the urban redevelopment project in Taipei, Taiwan. Taipei City Government has unveiled three new pavilions ("Pavilion of the Future", "Pavilion of Angel Life" and "Pavilion of Dreams" in the park for the 2010 Taipei International Flora Exposition. These pavilions were designed by the local architect Chang Ching-Hwa and constructed around old trees with their rooftops and walls populated by vegetation. After the expo, all fair pavilions were arranged to serve as activity venues for public events. During the park renewal, considerable endeavors were made to preserve the original condition of the park with main improvements of adding more green areas. The key vegetation design factors with different greening types were to have a positive impact on users' comfort level by decreasing the air temperature. Fig. 1 demonstrates the aero-photographs of

An-Shik Yang is with Department of Energy and Refrigerating Air-Conditioning Engineering, National Taipei University of Technology, Taipei 10608, Taiwan (phone: 886-2-2771-2171 ext. 3523; fax: 886-2-2731-49191; e-mail: asyang@ntut.edu.tw).

Chih-Yung Wen and Yu-Hsuan Juan are with Department of Mechanical Engineering, The Hong Kong Polytechnic University, Hung Hom, Kowloon, Hong Kong (phone: 852-2766-6657; fax: 852-2365-47031; e-mail: cywen@polyu.edu.hk).

Chiang-Ho Cheng is with the Department of Mechanical and Automation Engineering, University of Dayeh, Changhua 51591, Taiwan, (phone: 886-4-851-1888 ext. 2119; fax: 886-4-851-1224; e-mail: chcheng@mail.dyu.edu.tw).

the Taipei city and the photographs of featured scenic sites for three pavilions (Dreams, Angel Life and Future) in Xinsheng Park. It is located in northern Taiwan (25°04'16.1"N and 121°31'53.0"E) and is the second largest urban public park in Taipei, covering an area of 19.5 hectares. Taipei has a humid and subtropical climate. The meteorological data shows the coldest and warmest months are January and July, with the mean temperatures of 16.1 and 30.4 °C, respectively. In addition, the past study has found that the urban heat maximum in Taipei occurs at noon in summertime, with a heat island intensity of 4.9 K [10]. Therefore, this paper will focus on the microclimate study of the Xinsheng Park in July.

Fig. 1 Aero-photos of the Taipei city and three pavilions of Xinsheng Park

III. Computational Analysis

To conduct the digital analysis for predicting the comfort level of the outdoor wind environment, this investigation considers the ambient wind flowing over three pavilions of the Xinsheng Park in Taipei Flora Expo. The modeling software SolidWorks® was further employed to refine the solid model for preserving the buildings details. The exact shapes were precisely recreated using their real dimensions of the full-scale building from two- and three-dimensional architectural design drawings in an AutoCAD® data file format. The solid model was then readily transferred to the preprocessor of the CFD software ANSYS/Fluent® for flow was used to model the related atmospheric processes. Numerical computations by the ANSYS/Fluent® were performed to resolve the wind field structure characterized by the interaction between buildings and vegetation. The computational analysis was based on the steady-state three-dimensional conservation equations of mass, momentum and energy for the incompressible turbulent flow with the governing equations given as:

$$\frac{\partial u_i}{\partial x_i} = 0. \tag{1}$$

$$\frac{\partial \rho u_i u_j}{\partial x_j} = -\frac{\partial p}{\partial x_i} + \frac{\partial}{\partial x_j}\left[(\mu + \mu_t)\left(\frac{\partial u_i}{\partial x_j} + \frac{\partial u_j}{\partial x_i}\right)\right] + \rho_{ref} g_i \beta\left(T - T_{ref}\right) + S. \tag{2}$$

u_i represents the velocity component in the i axis; p, ρ, T, μ, μ_t, g_i and S_{ui} signify the pressure, density, temperature, dynamic viscosity, turbulent viscosity, gravity acceleration and source term describing the loss of wind speed owing to drag forces from plants, respectively. The present model treats density as a constant value in all equations, except for the buoyancy term in the momentum equation. The Boussinesq approximation, $\rho = \rho_{ref}\,\beta\,(T - T_{ref})$ in (2), was implemented to characterize the buoyancy-driven flow [11]. The properties of air at 30.4 °C (the mean radiation temperature of Xinsheng Park from 10:00-17:00 h, 14 July 2014) and 1 atm were applied to thermo-flow simulations. Moreover, the energy equation can be written in terms of sensible enthalpy h as

$$\frac{\partial \rho u_j h}{\partial x_j} = \frac{\partial}{\partial x_j}\left[(\lambda + \lambda_t)\left(\frac{\partial T}{\partial x_j}\right)\right] + \tau_{ij}\frac{\partial u_i}{\partial x_j} + S_h. \tag{3}$$

The terms λ and λ_t are the molecular and turbulent conductivity, τ_{ij} the deviatoric stress tensor, and S_h the energy source term relating heat exchange at the plant surface to the atmosphere. The detailed description of S_h will be given later.

To select the turbulent model, the realizable k-ε model, developed by Shih et al., has demonstrated its substantial improvements over the standard k-ε model for simulating the flows involving separation, vortices, rotation, and recirculation [12], [13]. In this work, the intricate geometry of the urban park in the core of Taipei city suggested the complex flow phenomena, and thus the realizable k-ε model was adopted for turbulence closure, as:

$$\frac{\partial \rho u_i k}{\partial x_i} = \mu_t S^2 - \rho\varepsilon + \frac{\partial}{\partial x_i}\left[\left(\mu + \frac{\mu_t}{\sigma_k}\right)\frac{\partial k}{\partial x_i}\right] + S. \tag{4}$$

$$\frac{\partial \rho u_i \varepsilon}{\partial x_i} = C_1 S\rho\varepsilon - C_2\frac{\rho\varepsilon^2}{k + \sqrt{\nu\varepsilon}} + \frac{\partial}{\partial x_i}\left[\left(\mu + \frac{\mu_t}{\sigma_\varepsilon}\right)\frac{\partial \varepsilon}{\partial x_i}\right] + S. \tag{5}$$

where μ_t is $C_\mu\,\rho k^2/\varepsilon$, k the turbulent kinetic energy, ε the turbulent energy dissipation rate and the variable $S = (2S_{ij}S_{ij})^{0.5}$ with $S_{ij} = 0.5(\partial u_i/\partial x_j + \partial u_j/\partial x_i)$. The factor $C_1 = \max[0.43, \eta/(\eta+5)]$ and $\eta = S(k/\varepsilon)$. The constants C_2, σ_k and $\sigma_\varepsilon$were given as 1.0, 1.0 and 1.2, respectively. The density, viscosity and conductivity of air are 1.163 kg/m^3, 1.877×10^{-5} N-s/m^2 and 0.0265 W/m-k at the mean temperature of 30.4 °C.

In simulations, the vegetation cover was modeled as porous medium to interact with the airflow. Specifically, the source terms were added to the transport equations in (2)-(5) to account for the effects of vegetation on the airflow and temperature. In (2), the local source term Sui can be expressed as [14]:

$$S_{u_i} = -\frac{1}{2}\rho \cdot C_d \cdot LAD \cdot u_i \cdot u. \tag{6}$$

where C_d the drag coefficient of plant elements with a specified value of 0.2, u the velocity magnitude and *LAD* the leaf area density in m^{2}m^{-3} of the plant. Four types of trees are planted in different parts of the park: *Sterculia foetida, Dillenia indica, Ficus microcarpa* and *Ficus benjamina*. These trees have been successfully used as street trees in various designed urban tree systems in Taiwan. The *Sterculia foetida* is a large, straight, deciduous tree that can grow up to a height of 20 m or more. The *Dillenia indica* is a medium sized deciduous tree. The

Ficus microcarpa is a lush and very popular evergreen tree. The *Ficus benjamina,* which is 30 m tall in natural conditions and commonly known as the weeping fig, makes itself a very large and stately tree for parks and other urban environments, such as wide roads. All four vegetation species were parameterized with the observed LAD profiles of formed plants. These data were then written into the User- Defined-Functions (UDFs) to characterize the three-dimensional canopy of the greening features in CFD simulations [15]. In the energy conservation equation, the source term S_h is used to relate heat exchange at the plant surface to the atmosphere and is modeled as [4]:

$$S_h = LAD \cdot J_{f,h}. \tag{7}$$

$$J_{f,h} = 1.1\ r_a^{-1}(T_f - T_a). \tag{8}$$

$$r_a = A(D/W)^{0.5}. \tag{9}$$

where the symbol $J_{f,h}$ is the direct heat flux, T_a the temperature of the air and T_f the foliage temperature. The aerodynamic resistance r_a is a function of the leaf geometry and wind speed, where W is the wind speed at the leaf surface. The values of the parameter A are 87 and 200 $s^{0.5}m^{-1}$ for grass and trees, respectively. D is the typical leaf diameter, ranging from 2 to 7 cm [4]. In (4) and (5), the local source terms S_k and S_ε model the generation and the dissipation of turbulence by the plants. It can be expressed by [16]:

$$S_k = \rho \cdot C_d \cdot LAD \cdot u_i^3. \tag{10}$$

$$S_\varepsilon = \frac{\varepsilon}{k} \cdot \rho \cdot C_d \cdot LAD \cdot u. \tag{11}$$

Equations (6), (7), (10) and (11) for modeling the effects of vegetation on air flow and temperature were implemented as the UDFs in CFD simulations [17].

This research treated the atmospheric boundary layer (ABL) flow to simulate the related atmospheric processes at the inflow boundary [18]. From a local meteorological station, the wind rose chart around Xinsheng Park at a height of 10 m in July 2014. In view of the wind conditions in terms of the speed, direction and probability, the wind speed occurred most frequently at 4.85 m/s from the south east (113°) of Xinsheng Park on July 17, 2014, which was used to calculate the neutral ABL velocity, U_{ABL}, turbulent kinetic energy, k, and turbulence dissipation rate profiles, ε, as the incoming wind flow conditions at the inlet of the computational domain [19], [20].

$$U_{ABL} = \frac{u^*_{ABL}}{K} \ln\left(\frac{z + z_0}{z_0}\right). \tag{12}$$

$$k = \frac{(u^*_{ABL})^2}{\sqrt{C_u}}. \tag{13}$$

$$\varepsilon = \frac{(u^*_{ABL})^3}{K(z + z_0)}. \tag{14}$$

The ABL friction velocity u^*_{ABL} can be computed from a specified velocity Uh at a reference height h as:

$$u^*_{ABL} = \frac{KU_h}{\ln\left(\frac{h + z_0}{z_0}\right)}. \tag{14}$$

The symbols z_0 and K stand for the aerodynamic roughness and the von Karman's constant (≈ 0.4). Equations (12)-(14) were applied to generate the mean inlet velocity at the height of z (U_{ABL}), the turbulence kinetic energy (k) and dissipation rate (ε) profiles within the ABL. In essence, roughness can increase the drag when the wind crosses the terrain surface, causing that the logarithmic law for the velocity profile, being the basis of the standard wall function approach, is incorrect in the presence of roughness [21]. In the ANSYS Fluent® software, the effect of real blockages on the wind was modeled by the roughness wall function setup to simulate the drags (from barriers) applied to the bottom surface. In consideration of the area bordering Xinsheng Park, the aerodynamic roughness was prescribed to be 2 m (z_0) based on the updated Davenport roughness classification for the city center with a complex involving high-rises and low-rise concrete frame mixed-use commercial and residential buildings [22].

In the present study, the radiation heat fluxes have to be considered in the simulations to correctly determine the wall surface temperatures, because the radiation influence can be crucial as compared to the heat transfer rates from convection or conduction. Hence, solar radiation was determined using the solar irradiation calculator of ANSYS Fluent®, which imposed the incident radiation on the exposed surfaces according to the sun position, varying with respect to the time, date and global location. Given that the geological coordinates of Xinsheng Park are at the latitude of 25°04'16.1"N and longitude of 121°31'53.0"E, the variations of total solar irradiation on July 17, 2014. Besides, the solar load model's discrete ordinates (DO) irradiation option in ANSYS Fluent® was employed. The solar irradiation was straightly applied to the DO model to determine the radiant heat fluxes between the surfaces of the computational domain through solving the radiation intensity transport equations (RTEs) for gray diffuse walls. The structures in the park were made of concrete, and the street was covered with asphalt in calculations. The spectral optical properties and thermos-physical properties of involved materials were given in [23]. The air emissivity of external field ε_{ext} was set as 0.05 with the external radiation temperature of 36.5 °C. Besides, the heat transfer coefficients (h_c) of building surfaces were evaluated via the following empirical correlation, which is independent of the wind direction and is suitable for high wind velocities [24]:

$$h_c = 5.7 + 3.8V_{air}. \tag{9}$$

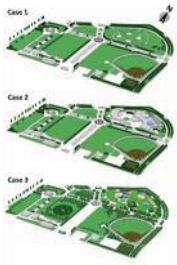

Model Area, %	Case 1	Case 2	Case 3
Building coverage	16.9	30.7	16.8
Tree coverage	17.5	14.9	21.9
Grass coverage	48.9	39.6	35.8
Green roof coverage	-	-	13.9
Ground	16.7	14.8	11.1
Total	100	100	100

Fig. 2 Three cases of greening and associated coverage ratios

Here V_{air} is the airflow velocity. In simulations, the plant was considered to be semi-transparent in the radiative model. Part of the solar radiation incident on the tree was reflected, whereas another part tended to penetrate through the tree canopy with occurrence of absorption and transmission of radiation [14].

To treat the boundary conditions at the outlet, the constant static pressure (1 atm) was employed at the exit of the calculation domain. The zero normal gradients of *p, k* and *ε* were imposed on the solid surface, with the log-law wall functions applied for the next-to-surface grids of buildings [24]. The top and lateral boundaries were placed at 10 H from the ground and 1.5 W from the centerline of computational domain, where H and W were the maximum height of object buildings and the width of built area, respectively. The symmetry boundary conditions were employed by prescribing the zero normal component of velocity and zero normal derivatives for all flow variables at the top and lateral boundaries.

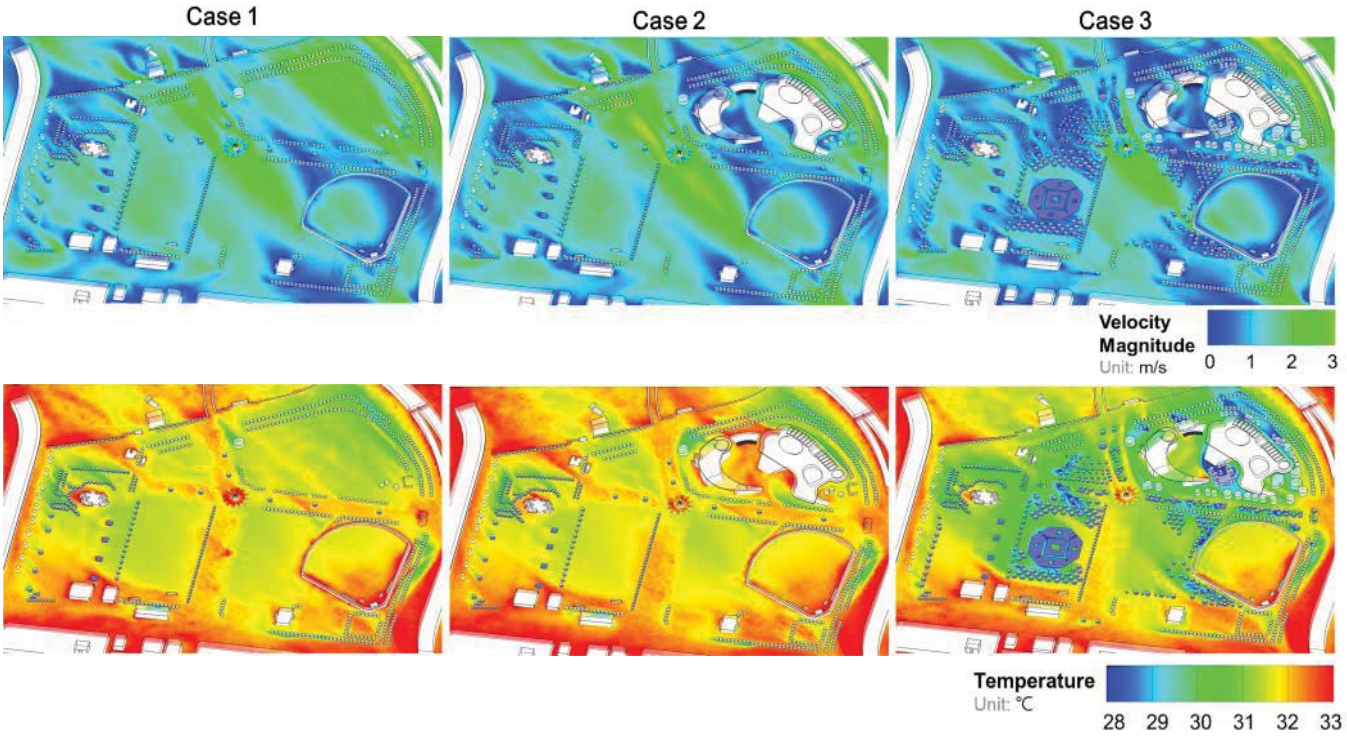

Fig. 3 Predicted velocity magnitude and temperature contours at a height of 1.75 m

The aforesaid mathematical equations were discretized by the finite control volume approach. This study used a second-order accurate central difference scheme to model the convective terms with adaptive damping for handling non-physical oscillations. To appraise the diffusion terms, a second-order accurate central difference scheme was employed in numerical solutions. An iterative semi-implicit method for pressure-linked equations consistent (SIMPLEC) numerical method was used for velocity-pressure coupling [25]. A steady solution was obtained with convergence of the normalized residual errors of flow variables (*u, v, w, p, T, k* and *ε*) to 10^{-5} and the mass balance check lower than 1% for achieving the wind field environments.

IV. Results and Discussion

This research attempted to simulate realistic urbanized environs with detailed geometries of buildings and street canyons for exploring the vegetation covering effect on the associated flow and thermal processes. The CFD simulations were conducted using the ANSYS/Fluent® and the present computational model was validated by comparing the predictions with the measurement results. The geometric dimensions of 230 m long, 170 m wide and 16 m average high for three pavilions. For the mesh system modeling a representative public building in urbanized area, the averaged cell size was around 0.63 m with the least spacing of 0.019 m to resolve steep variations of flow properties associated with the interaction of airflow with buildings. In this research, numerical computations were performed on the total number grids of 63157691. In this investigation, we illustrated the CFD simulation results of outdoor and indoor airflow characteristics

to appraise the quality of ventilation. In view of the wind flowing over the target buildings from the east side of the Xinsheng Park during the exhibition period in the summer weather conditions, this research analyzes the general wind environment around three pavilions at the pedestrian plane of 1.5 m high of the pavilions of Future and Angel Life. CFD simulations were conducted to examine the effects of cooling potential for different greening modifications on urban microclimates by considering the original form of Xinsheng Park (before renewal) as Case 1, addition of three pavilions to the park (after renewal) as Case 2, and realization of the supplementary green areas as Case 3 (the current form). Fig. 2 exhibits three cases showing various types of greening and the related coverage ratios with Case 1 as the baseline condition. In this case, trees/shrubs and grasses enveloped 17.5% and 48.9% of the total ground area, respectively, corresponding to a green coverage ratio (GCR) of 66.4%. In Case 2, three pavilions were constructed in the park with only limited existing vegetated areas removed to attain a GCR of 54.5%, whereas the overall GCR of the park increased to 71.6% by planting more trees and cultivating the grass on the roofs of three pavilions in Case 3.

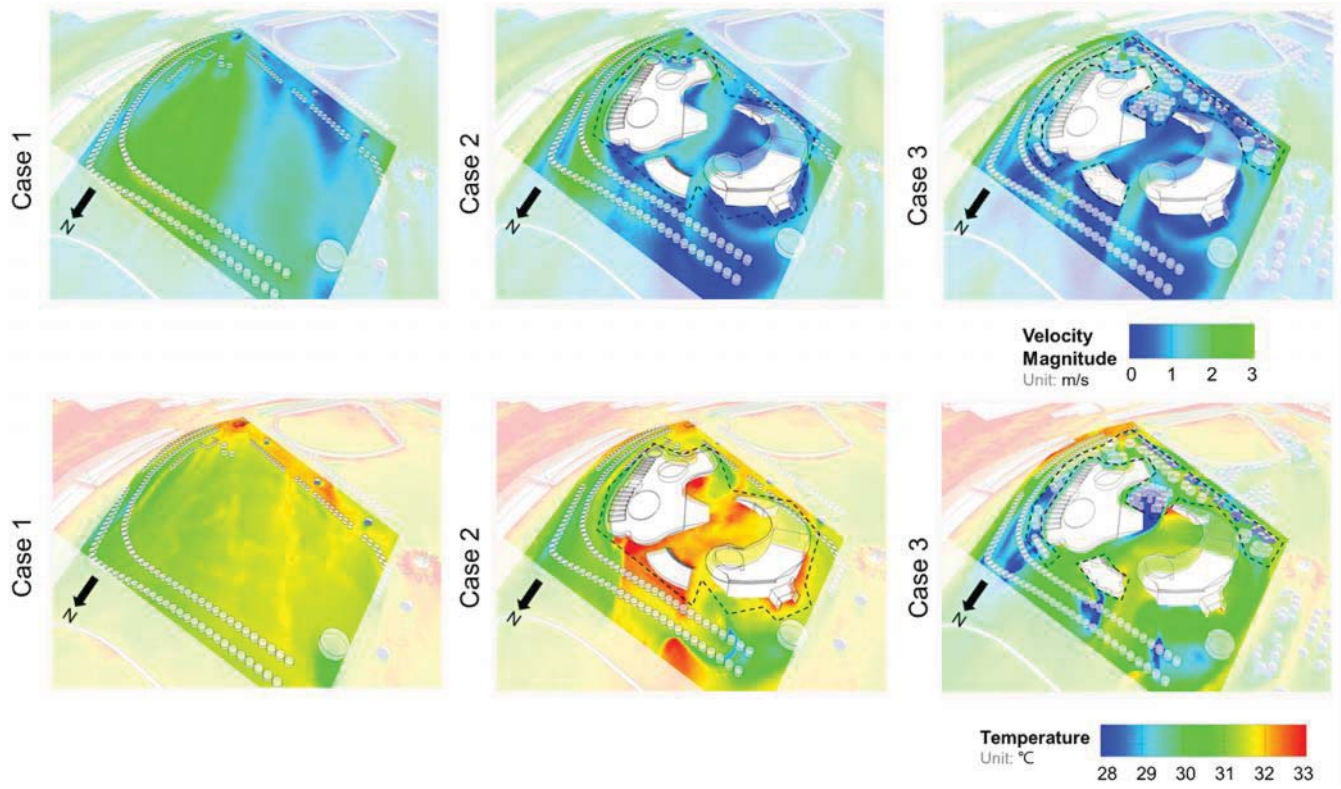

Fig. 4 Predicted velocity magnitude and temperature contours at a height of 1.75 m

Fig. 3 illustrates the predicted results of velocity magnitude and temperature contours at a height of 1.75 m in the pedestrian level. The simulated results were used to better understand the influences of different greening modifications on the thermal and flow fields in the park renewal process. The color bar charts of the velocity magnitude and temperature contours were retained in the same ranges for easier comparison. Considering the airflow blowing over Xinsheng Park from the south east at a speed of 4.85 m/s, the predicted velocity distribution at the pedestrian level before park renewal revealed that the fresh airflow entering the park was partially blocked by a baseball field with the wind speed ranging from 0.4 to 1.7 m/son both sides of the audience area. High velocities up to 3 m/s (in a green color) were observed in the center and upper right region of the park owing to the relatively lower flow resistance of flat ground surfaces. In Case 2, high velocities merely appeared in the mid park with significant velocity decrease occurred around three pavilions. In Case 3, an increase in flow resistance resulting from supplementary plants caused a drop of the airflow speed ranging approximately 0.3-1.5 m/s in those green areas (i.e. a labyrinth and a cluster of bushes). In consideration of the outdoor thermal environments, it was observed that the presence of three pavilions in Case 2 produced elevated temperatures (to around 32-33˚C), as compared to the temperatures of 30.6-31.8˚C for the scenario without built structures in Case 1. Furthermore, the CFD predictions obviously revealed the reduction of temperature to 28.8-31.3°C after adding the aforementioned green areas of trees and other plants to cool the environment in Case 3, making vegetation a simple and useful way to lessen urban heat islands.

Numerical calculations were further conducted to achieve a better understanding of the outdoor thermo-flow environments for three zones of Xinsheng Park. In Fig. 4, illustrating the CFD predictions in Zone 3, the wind speed and temperature ranged 1-3 m/s and 30-32°C over a large unused flat area without built structures in Case 1. For the scenario of constructing three

pavilions during park renewal (in Case 2), the predictions obviously revealed substantial reduction of the wind speed to 0.5-2.3 m/s because of the blocking outcome of three pavilions. On the other hand, the outdoor temperatures were increased up to 33°C in consequence of the straight exposure to solar radiation and lack of greenery in that area. Although the wind speed distributions for Case 2 and 3 were similar, the computed results of Case 3 revealed a notable temperature difference between the states with and without planting trees and grasses around the pavilions. The ambient temperatures were reduced to 29.1-31.4°C due to additional green areas, as compared to those in Case 2.

V. Conclusion

The objective of this study was to investigate the influences of vegetation on the improvement of urban microclimates after the renewal of a public park (Xinsheng Park) in Taipei, Taiwan. Numerical simulations and field measurements were performed to examine the thermo-flow behaviors in the Xinsheng Park, allowing architects and planners to better understand the impacts of the park design through adding three pavilions and supplementary green areas on urban microclimates for decision support. The major results are summarized as below: From the predicted velocity magnitude and temperature contours, it can be seen that trees and vegetation are effective to provide shading from solar radiation to buildings, and accordingly reduce surface temperatures of the environments. The average temperature was reduced by 2.42°C to achieve a cooler locality by augmented tree/grass coverage ratios of 4.3/21.8%. The findings suggest a useful measure via implementing greening modifications in public parks to enhance cooling result for mitigation of urban heat island effect in Taipei, Taiwan.

Acknowledgment

This study represents part of the results obtained under the support of National Science Council, Taiwan, ROC (Contract No. NSC101-2627-E-027-001-MY3).

References

[1] E. Ng, L. Chen, Y. Wang, C. Yuan, A study on the cooling effects of greening in a high-density city: An experience from Hong Kong, *Building and Environment*, 47 (2012), 256-271.

[2] A.H. Rosenfeld, H. Akbari, S. Bretz, B.L. Fishman, D.M. Kurn, D. Sailor, H. Taha, Mitigation of urban heat islands: Materials, utility programs, updates. *Journal of Energy and Buildings,* 22 (1995) 255–265.

[3] H. Taha, Urban climates and heat islands: albedo, evapotranspiration, and anthropogenic heat, *Energy and Buildings*, 25 (1997) 99-103.

[4] M. Bruse, H. Fleer, Simulating surface–plant–air interactions inside urban environments with a three dimensional numerical model, *Environmental Modelling & Software,* 13 (1998) 373-384.

[5] A.Dimoudi, M. Nikolopoulou, Vegetation in the urban environment: microclimatic analysis and benefits, *Energy and Buildings,* 35 (2003) 69-76.

[6] E. Alexandri, P. Jones, Temperature decreases in an urban canyon due to green walls and green roofs in diverse climates, *Building and En*vironment, 43 (2008) 4810-493.

[7] D. Fröhlich, A. Matzarakis , Modeling of changes in thermal bioclimate: examples based on urban spaces in Freiburg, Germany. *Theoretical and Applied Climatology*. 111 (2013) 547-558.

[8] B. Vidrih, S. Medved, Multiparametric model of urban park cooling island, *Urban Forestry & Urban Greening*, 12 (2013) 220-229.

[9] M. Srivanit, K. Hokao, Evaluating the cooling effects of greening for improving the outdoor thermal environment at an institutional campus in the summer, *Building and Environment*, 66 (2013) 158-172.

[10] H. T. Lin, K. P. Lee, K. T. Chen, L. J. Lin, H. C. Kuo, T. C. Chen, Experimental analyses of urban heat island effects of the four metropolitan cities in Taiwan (I) - The comparison of the heat island intensities between Taiwan and the world cities, *Journal of Architecture,* 31(1999) 51-73.

[11] M. Z.I. Bangalee, J. J. Miau, S. Y. Lin, J. H. Yang, Flow visualization, PIV measurement and CFD calculation for fluid-driven natural cross-ventilation in a scale model, *Energy and Buildings*, 66 (2013) 306-314.

[12] T. H. Shin, W. W. Liou, A. Shabbir, Z. Yang, J. Zhu, A new k-ε eddy viscosity model for high Reynolds number turbulent flows, *Computers Fluids,* 24 (1995) 227-238.

[13] P. Karava, C. M. Jubayer, E. Savory, Numerical modelling of forced convective heat transfer from the inclined windward roof of an isolated low-rise building with application to photovoltaic/thermal systems, *Applied Thermal Engineering*, 31 (2011) 1950-1963.

[14] M. Robitu, M. Musy, C. Inard, D. Groleau, Modeling the influence of vegetation and water pond on urban microclimate, *Solar Energy*, 80 (2006) 435-447.

[15] ANSYS Inc., ANSYS FLUENT 14.0 user's guide. ANSYS, Inc. United States, 2011.

[16] H. Barden, *Simulationsmodell für den Wasser-, Energie- und Stoffhaushalt in Pflanzenbeständen.,* Hannover, Inst. für Meteorologie u. Klimatologie d. Univ, 1982.

[17] Harrison RM. Understanding our environment: an introduction to environmental chemistry and pollution. Royal Society of Chemistry, Cambridge, UK; 1992.

[18] Blocken B, Carmeliet J, Stathopoulos T. CFD evaluation of wind speed conditions in passages between parallel buildings—effect of wall-function roughness modifications for the atmospheric boundary layer flow. J Wind Eng Ind Aerod 2007; 95:941-962.

[19] Richards PJ. Computational modelling of wind flows around low rise buildings using PHOENIX. Report for the ARFC Institute of Engineering Research Wrest Park, Bedfordshire, UK; 1989.

[20] Wieringa J. Updating the Davenport roughness classification. J Wind Eng Ind Aerod 1992; 41:357-368.

[21] Chen WF. Handbook of structural engineering. CRC Press, Boca Raton, Fla.; 1997.

[22] Hargreaves DM, Wright NG. On the use of the k– model in commercial CFD software to model the neutral atmospheric boundary layer. J Wind Eng Ind Aerod 2007;95:355-369.

[23] Fidaros DK, Baxevanou CA, Bartzanas T, Kittas C. Numerical simulation of thermal behavior of a ventilated arc greenhouse during a solar day. Renew Energ 2010;35:1380-1386.

[24] Palyvos JA. A survey of wind convection coefficient correlations for building envelope energy systems' modeling. Appl Therm Eng 2008; 28:801-808.

[25] Van Doormaal JP, Raithby GD. Enhancement of the SIMPLE Method for Predicting Incompressible Fluid Flows. Numer Heat Tr. 1984;7:147-163.

An-Shik Yang received his Bachelor of Science (1982) and Master of Science (1984) degrees from the National Tsing Hua University in Taiwan, and Ph.D. (1993) degree from the Pennsylvania State University in USA. He is currently a professor with the Department. of Energy and Refrigerating Air-Conditioning Engineering at National Taipei University of Technology (NTUT). Dr. Yang is an Associate Fellow of American Institute of Aeronautics and Astronautics (AIAA). His research interest is in the areas of environmental fluid mechanics, microfluidic design and heat transfer.

Chih-Yung Wen received his B.S. degree from the Department of Mechanical Engineering at the National Taiwan University in 1986 and M.S. and PhD from the Department of Aeronautics at the California Institute of Technology, U.S.A. in 1989 and 1994. He joined the Department of Mechanical Engineering, The Hong Kong PolyU in 2012 as professor. Professor Wen, currently an AIAA Associate Fellow, serves as a member of, various key professional boards and bodies related to the Aerospace Engineering.

Chiang-Ho Cheng joins the Department of Mechanical and Automation Engineering at Dayeh University as an associate professor on February 1999,

and was promoted to full professor in fall 2012. He earned his Ph.D. degree in Institute of Applied Mechanics from National Taiwan University in 1996. His research interests include the MEMS system, the design and analysis of piezoelectric droplet inkjets and micropumps.

Yu-Hsuan Juan received her bachelor degree in department of aerospace and systems engineering from the Feng Chia University in 2011 and got her master degree in department of energy and refrigerating air-conditioning engineering from National Taipei University of Technology in 2013. She is currently working as research assistant on the Department of Mechanical Engineering, The Hong Kong PolyUy. Her main research interests include the fluid dynamics of Environmental, heat transfer and numerical simulation analysis of microclimate.